



Article

Photon- and Singlet-Oxygen-Induced Cis–Trans Isomerization of the Water-Soluble Carotenoid Crocin

Franco Fusi ¹, Giovanni Romano ^{1,*}, Giovanna Speranza ² and Giovanni Agati ³

¹ Department of Experimental and Clinical Biomedical Sciences “Mario Serio”, University of Florence, Viale G. Pieraccini, 6, 50139 Florence, Italy; franco.fusi@unifi.it

² Department of Chemistry, University of Milan, Via Golgi 19, 20133 Milan, Italy; giovanna.speranza@unimi.it

³ “Nello Carrara” Institute of Applied Physics (IFAC), National Research Council (CNR),

Via Madonna del Piano 10, 50019 Sesto Fiorentino, Italy; g.agati@ifac.cnr.it

* Correspondence: giovanni.romano@unifi.it

Abstract: Studying the cis–trans isomerization process in crocin (CR), one of the few water-soluble carotenoids extracted from saffron, is important to better understand the physiological role of cis-carotenoids in vivo and their potential as antioxidants in therapeutic applications. For that, cis–trans isomerization of both methanol- and water-dissolved CR was induced by light or thermally generated singlet oxygen (¹O₂). The kinetics of molecular concentrations were monitored by both high-performance liquid chromatography (HPLC) and non-destructive spectrophotometric methods. These last made it possible to simultaneously follow the cis–trans isomerization, the possible bleaching of compounds and the amount of thermally generated ¹O₂. Our results were in accordance with a comprehensive model where the cis–trans isomerization occurs as relaxation from the triplet state of all-trans- or 13-cis-CR, whatever is the way to populate the CR triplet state, either by photon or ¹O₂ energy transfer. The process is much more (1.9 to 10-fold) efficient from cis to trans than vice versa. In H₂O, a ¹O₂-induced bleaching effect on the starting CR was not negligible. However, the CR “flip-flop” isomerization reaction could still occur, suggesting that this process can represent an efficient mechanism for quenching of reactive oxygen species (ROS) in vivo, with a limited need of carotenoid regeneration.

Keywords: crocin; differential absorbance; photoisomerization; quantum yields; quenching; singlet oxygen; Z-E isomers; antioxidant; crocin based assay CBA



Citation: Fusi, F.; Romano, G.; Speranza, G.; Agati, G. Photon- and Singlet-Oxygen-Induced Cis–Trans Isomerization of the Water-Soluble Carotenoid Crocin. *Int. J. Mol. Sci.* **2023**, *24*, 10783. <https://doi.org/10.3390/ijms241310783>

Academic Editors: Angela Scala, Antonino Mazzaglia and Enrico Caruso

Received: 30 May 2023
Revised: 20 June 2023
Accepted: 25 June 2023
Published: 28 June 2023



Copyright: © 2023 by the authors. Licensee MDPI, Basel, Switzerland. This article is an open access article distributed under the terms and conditions of the Creative Commons Attribution (CC BY) license (<https://creativecommons.org/licenses/by/4.0/>).

1. Introduction

Carotenoids are well known natural pigments utilized by photosynthetic systems in the light-harvesting as well as in the photoprotection mechanisms [1]. They easily undergo cis–trans isomerization; however, the biological functional role of the resulting different configurations has not been completely elucidated yet.

Normally carotenoids occur in nature as the all-trans isomer. However, cis configurations have also been isolated from several vegetables [2–4] and the *Dunaliella bardawil* green alga [2]. The differential localization of all-trans and 15-cis isomers of β-carotene in the photosynthetic apparatus of the *Rhodospirillum rubrum* S1 bacterium indicates a specific biological function of these compounds linked to their geometrical structure. In the reaction center, the presence of the 15-cis configuration, with a longer conjugated chain, is suggested to have a more efficient photoprotection role with respect to the all-trans isomer in dissipating the excess of energy. While the all-trans configuration, with a shorter conjugated chain, in the light-harvest complex provides an optimized excitation energy transfer to chlorophyll [5]. Therefore, cis–trans carotenoids are important actors in light absorption and membrane protection against ROS (singlet oxygen and free radicals) [1].

Cis-carotenes are also involved as molecular signals to control plastid activities and plant development [6], while the cis/trans isomer ratio in food has been seen to increase during processing [7]. On the other hand, the bioavailability of carotenoid cis-isomers and their accumulation in human serum and tissues was found to be higher than the all-trans-isomers [8,9]. This is likely due to the decreased tendency of cis-isomers to form aggregates and crystals [10].

The high efficiency of carotenoids in quenching singlet oxygen focused large interest on these molecules as antioxidant agents [11]. This property can also explain the in vivo observation of a positive role of carotenoids in the prevention of cancer [12], in delaying the progress of neurodegenerative diseases [13] and in providing other numerous health benefits [14].

Since the $^3\text{O}_2$ excitation energy to produce $^1\text{O}_2$ is $94.5 \text{ kJ}\cdot\text{mol}^{-1}$, $^1\text{O}_2$ can be easily produced in vivo by natural sensitizers (e.g., chlorophyll) and its production is followed by oxidation of several cellular components. This process can be significantly reduced by carotenoids able to physically quench $^1\text{O}_2$ by energy transfer [15] and also inducing the cis–trans isomerization [3].

The cis–trans interconversion is a well-known process that can be induced by light, directly or through a photosensitizer [16], as well as by high temperatures ($>70 \text{ }^\circ\text{C}$) [16,17].

High-performance liquid chromatography (HPLC) along with time-resolved Raman and absorption spectroscopy provided an accurate quantitative evaluation of β -carotene photoisomerization. The results showed that: (1) the cis–trans isomerization occurs as relaxation of the triplet excited state even in the case of direct photoisomerization; (2) the all-trans and 15-cis isomers have a common intermediate triplet state; (3) the isomerization of 15-cis is an order of magnitude more efficient than isomerization of all-trans [16,18,19].

Further evidence about the triplet-state-mediated photoisomerization route was also reported for zeaxanthin [20].

The isomerization reaction following $^1\text{O}_2$ quenching by carotenoids is much less studied.

More than fifty years ago, it was first observed that $^1\text{O}_2$ can sensitize the 15-cis to all-trans- β -carotene isomerization [21]. In that study, based only on absorption spectroscopy, no appreciable inverse trans-to-cis process was observed. Much later, Heymann et al. [3] clearly showed that $^1\text{O}_2$ can produce different cis isomers, starting the reaction from the all-trans configuration in both lycopene and β -carotene.

Several authors reported data on the physical and chemical $^1\text{O}_2$ -quenching rate constants of several trans and cis carotenoids [15,22–25]. However, the reaction models used did not consider the potential contribution to the quenching rates of the cis–trans isomerization.

Most of the carotenoid isomerization processes have been extensively studied in non-polar organic solvents, in which they possess a high solubility. In this environment, carotenoids are able to quench singlet oxygen physically rather than chemically [22].

In some studies, conducted in aqueous media by using reverse micelle systems, a large difference of four orders of magnitude between the physical and chemical $^1\text{O}_2$ quenching rate constants of carotenoids was still found [26,27].

Information on the photophysical and chemical properties of water-soluble carotenoids is relevant to the understanding of the protective role they play in vivo in the photodynamic oxidation of biological systems.

In the presence of high concentrations of ROS, the organism can use exogenous antioxidants supplied with the diet or through pharmaceutical products. To characterize an antioxidant compound, it is necessary to consider the mechanisms involved and therefore both the activity and the antioxidant capacity. Antioxidant activity refers to the rate constant of a reaction between an antioxidant and an oxidant. Antioxidant capacity is a measure of the amount of a certain free radical captured by an antioxidant sample.

In the literature [28], an in vitro method (CBA- Crocin Based Assay) is presented for measuring the antioxidant and prooxidant capacity of nutritional supplements, pharmaceuticals and biological samples, based on a hydro-soluble carotenoid.

Crocin (CR) [29] is the major pigment of saffron, the spice obtained from the dried stigmata of *Crocus sativus* L., to whom it confers the characteristic yellow color. Being a water-soluble carotenoid, it is a unique antioxidant. It is used in the treatment of many diseases [30] and for cytoprotective properties, including systemic [31] or local [32] anti-inflammatory effect.

Only few studies on photochemical and $^1\text{O}_2$ -induced reactions in water-soluble carotenoids, such as 8,8'-diapocarotene-8,8'-dioic acid (crocetin) [23,33], its digentiobiosyl ester (CR) [23,34,35] and a series of 6,6'-diapocarotenoids [25,34], have been reported.

In the present paper, we report a complete investigation on the cis-trans isomerization of all-trans- and 13-cis-CR (Figure 1) induced by photon or by energy transfer from singlet oxygen in methanol as well as aqueous solutions. A spectroscopic method for the contemporary detection of $^1\text{O}_2$ production, carotenoid bleaching and isomerization is proposed. Additional quantitative information on the trans/cis isomer concentrations during the reaction processes were obtained by HPLC analysis.

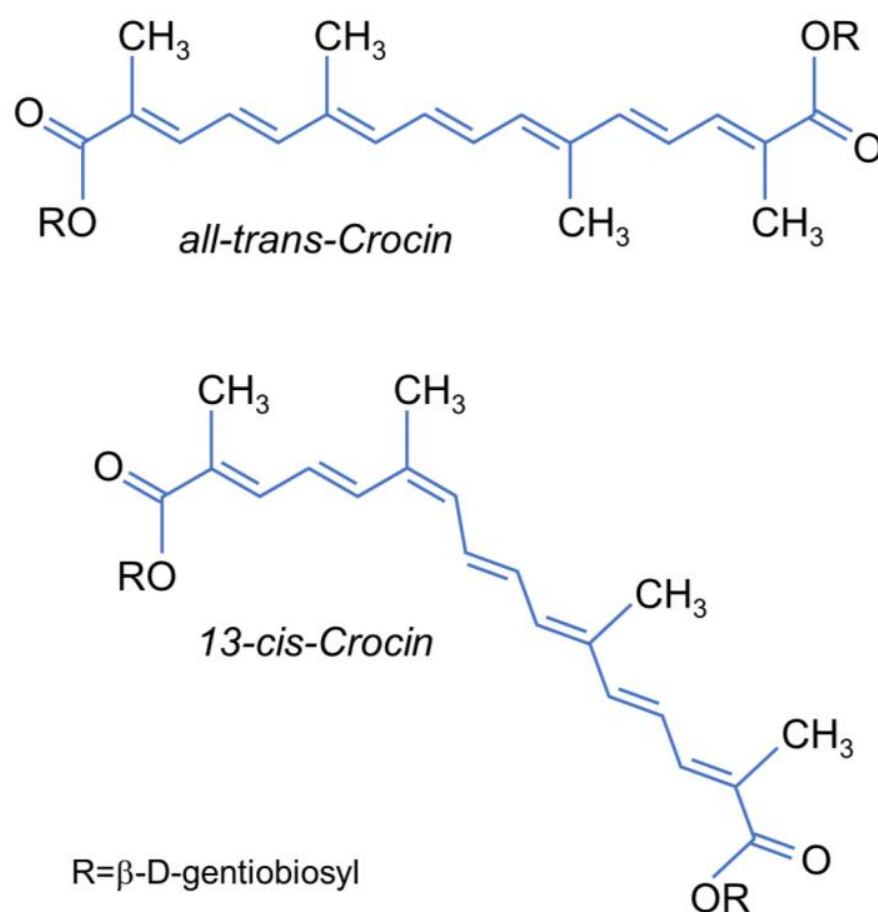


Figure 1. Chemical structure of all-trans- and 13-cis-crocin.

2. Results

Based on the actual knowledge about the way to induce the cis-trans isomerization in carotenoid molecules [16,20], we schematized the possible processes occurring in CR, as reported in Figure 2.

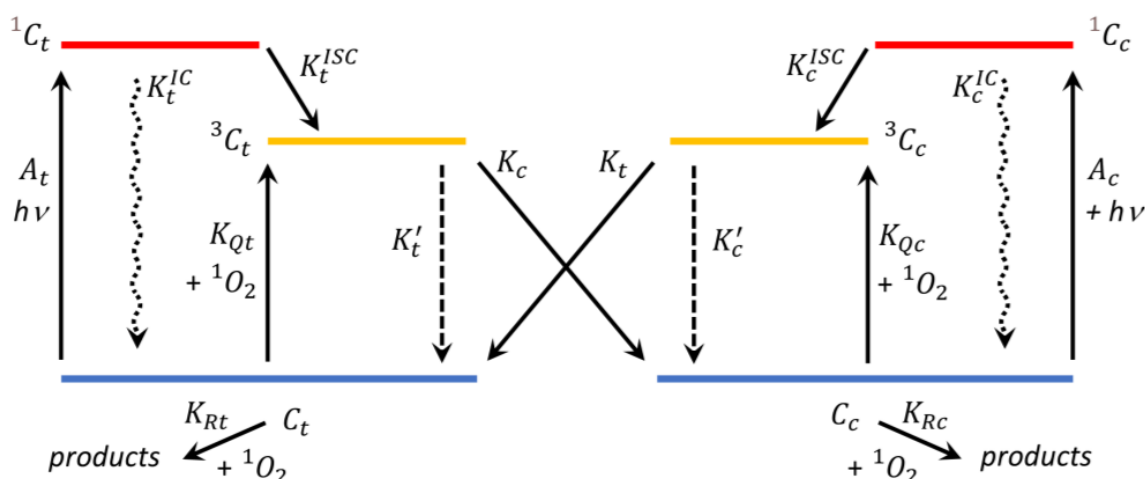


Figure 2. Scheme of the main photochemical and $^1\text{O}_2$ -induced trans-cis isomerization processes in crocin. A_t and A_c are the excitation rate constants from the steady state of all-trans-CR (C_t) and 13-cis-CR (C_c), respectively, to their singlet excited states, 1C_t and 1C_c , respectively. The K_t^{IC} and K_c^{IC} are the rate constants for the internal conversion from singlet excited- to ground-states; the K_t^{ISC} and K_c^{ISC} are the rate constants for the intersystem crossing to generate the triplet energy states, 3C_t and 3C_c of C_t and C_c , respectively. $K_{Q_{t,c}}$ and $K_{R_{t,c}}$ are the bimolecular rate constants for physical and chemical quenching of $^1\text{O}_2$, respectively. The deexcitation rates of the CR triplet states are indicated by K_t and K_c for the trans \leftrightarrow cis isomerization processes and by K_t' and K_c' for the internal relaxation processes.

2.1. Kinetics of the all-trans \leftrightarrow 13-cis Photoreaction

According to the scheme reported in Figure 2, the kinetics of the all-trans \leftrightarrow 13-cis photoreaction during monochromatic irradiation at the λ_i wavelength, neglecting any photobleaching, is described by the following equation:

$$\begin{aligned}
 \dot{C}_t &= -A_t C_t + K_t^{IC} {}^1C_t + K_t' {}^3C_t + K_t {}^3C_c \\
 {}^1\dot{C}_t &= A_t C_t - (K_t^{IC} + K_t^{ISC}) {}^1C_t \\
 {}^3\dot{C}_t &= K_t^{ISC} {}^1C_t - (K_c + K_t') {}^3C_t \\
 \dot{C}_c &= -A_c C_c + K_c^{IC} {}^1C_c + K_c' {}^3C_c + K_c {}^3C_t \\
 {}^1\dot{C}_c &= A_c C_c - (K_c^{IC} + K_c^{ISC}) {}^1C_c \\
 {}^3\dot{C}_c &= K_c^{ISC} {}^1C_c - (K_t + K_c') {}^3C_c \\
 \frac{C_t + C_c}{C_0} &= 1
 \end{aligned} \quad (1)$$

where C_t and C_c denote the concentrations of the all-trans and 13-cis isomers in the ground state, respectively, and C_0 is the initial concentration of the solution. The 1, 3 superscript numbers of concentrations mean singlet- and triplet-excited states; the dot apices indicate the time derivatives of populations; and the light excitation of ground-state molecules to the singlet excited states is driven by the rate constants.

$$A_t = \sigma_t(\lambda_i) \cdot F; \quad A_c = \sigma_c(\lambda_i) \cdot F \quad (2)$$

where $\sigma_t(\lambda_i)$ and $\sigma_c(\lambda_i)$ represent the absorption cross-sections of all-trans and 13-cis, respectively, and F denotes the incident photon fluence rate.

Equations (1) and (2) are valid in the limit of an optically thin solution, $\alpha l \ll 1$, with α and l denoting the absorption coefficient and the thickness of the solution, respectively.

Over the thickness l of the solution with the absorption coefficient α , the spatial average of F is

$$\langle F \rangle = \frac{F}{l} \int_0^l e^{-\alpha x} dx = F \cdot \frac{(1 - e^{-\alpha l})}{\alpha l} \quad (3)$$

The averaged F value was considered in the following equations to give a more accurate determination of the photoisomerization quantum yields (Equation (13)), even if in our case F variations along the light path are of the order of 5–15% and could be neglected. Within the steady-state approximation, ${}^1\dot{C}_t = {}^3\dot{C}_t = {}^1\dot{C}_c = {}^3\dot{C}_c = 0$, we have that

$$\begin{aligned} {}^1C_t &= \frac{A_t C_t}{K_t^{IC} + K_t^{ISC}}; \quad {}^1C_c = \frac{A_c C_c}{K_c^{IC} + K_c^{ISC}} \\ {}^3C_t &= \frac{A_t C_t \cdot K_t^{ISC}}{(K_t^{IC} + K_t^{ISC}) \cdot (K_c + K_t')} ; \quad {}^3C_c = \frac{A_c C_c \cdot K_c^{ISC}}{(K_c^{IC} + K_c^{ISC}) \cdot (K_t + K_c')} \end{aligned} \quad (4)$$

that combined with Equation (1) lead to

$$\begin{aligned} \dot{C}_t &= -Y_c \Phi_t^{ISC} A_t C_t + Y_t \Phi_c^{ISC} A_c C_c = -\phi_c A_t C_t + \phi_t A_c C_c \\ \dot{C}_c &= -Y_t \Phi_c^{ISC} A_c C_c + Y_c \Phi_t^{ISC} A_t C_t = -\phi_t A_c C_c + \phi_c A_t C_t \end{aligned} \quad (5)$$

with

$$Y_c = \frac{K_c}{K_c + K_t'} ; \quad Y_t = \frac{K_t}{K_t + K_c'} \quad (6)$$

defined as the yields of isomerization from trans to cis (Y_c) and vice versa (Y_t), respectively, and

$$\Phi_t^{ISC} = \frac{K_t^{ISC}}{(K_t^{IC} + K_t^{ISC})} ; \quad \Phi_c^{ISC} = \frac{K_c^{ISC}}{(K_c^{IC} + K_c^{ISC})} \quad (7)$$

are the triplet-state quantum yields through intersystem crossing for all-trans- and 13-cis-CR, respectively.

We can then define the quantum yields of all-trans to 13-cis photoisomerization, and vice versa from 13-cis to all-trans, as the product of the triplet-state quantum yields by the yield of isomerization from the triplet state:

$$\phi_c = Y_c \Phi_t^{ISC} ; \quad \phi_t = Y_t \Phi_c^{ISC} \quad (8)$$

Starting the irradiation, at λ_i , of a CR solution, the time evolution of the relative concentration of CR isomers, defined as $c_{t,c} = C_{t,c}/C_0$, which satisfy the initial conditions, at $t = 0$, $c_t(0) = 1$ and $c_c(0) = 0$ are given as solutions of the system (5):

$$\begin{aligned} c_t(t) &= c_t(\infty) + c_c(\infty) \cdot e^{-\frac{t}{\tau}} \\ c_c(t) &= c_c(\infty) (1 - e^{-\frac{t}{\tau}}) \end{aligned} \quad (9)$$

where

$$\begin{aligned} c_t(\infty) &= \left(1 + \frac{Y_c \Phi_t^{ISC} \sigma_t}{Y_t \Phi_c^{ISC} \sigma_c} \right)^{-1} = \left(1 + \frac{\phi_c \sigma_t}{\phi_t \sigma_c} \right)^{-1} \\ c_c(\infty) &= \left(1 + \frac{Y_t \Phi_c^{ISC} \sigma_c}{Y_c \Phi_t^{ISC} \sigma_t} \right)^{-1} = \left(1 + \frac{\phi_t \sigma_c}{\phi_c \sigma_t} \right)^{-1} \end{aligned} \quad (10)$$

are the relative concentrations of the two isomers at the photoequilibrium, with

$$\tau^{-1} = \langle F \rangle (\phi_t \sigma_c + \phi_c \sigma_t) \quad (11)$$

and combining the two expressions in Equation (10), we obtain

$$\frac{\phi_t}{\phi_c} = \frac{c_t(\infty)}{c_c(\infty)} \cdot \frac{\sigma_t}{\sigma_c} = \frac{c_t(\infty)}{c_c(\infty)} \cdot \frac{\varepsilon_t}{\varepsilon_c} \left(\text{being } \varepsilon = \frac{Na}{\ln 10} \sigma \right) \quad (12)$$

At the initial stage of the all-trans to 13-cis photoisomerization and vice versa, around $t = 0$, from Equation (5) we can calculate the quantum yields

$$\begin{aligned}\phi_c &= \frac{-\dot{C}_t}{\sigma_t(F)C_t(0)} = \frac{-\dot{c}_t}{\sigma_t(F)} = \frac{\tau^{-1}c_c(\infty)}{\sigma_t(F)} \\ \phi_t &= \frac{-\dot{C}_c}{\sigma_c(F)C_c(0)} = \frac{-\dot{c}_c}{\sigma_c(F)} = \frac{\tau^{-1}c_t(\infty)}{\sigma_t(F)}\end{aligned}\quad (13)$$

where the right-end expressions were obtained by calculating the first derivative in the origin of Equation (9).

In the trans–cis photoisomerization process, and in the absence of any photobleaching, the absorption coefficient of the CR solution as a function of time and wavelength is given by

$$\alpha(t, \lambda) = C_0(\sigma_t(\lambda) \cdot c_t(t) + \sigma_c(\lambda) \cdot c_c(t)) \quad (14)$$

where C_0 represents the initial concentration of CR molecules.

As a result, during the irradiation of a solution of all-trans-CR (or 13-cis-CR), the difference absorption coefficient $\Delta\alpha(t, \lambda)$ evolves concurrently with c_c (or c_t):

$$\Delta\alpha(t, \lambda) = \alpha(t, \lambda) - \alpha(0, \lambda) = \alpha(0, \lambda) \cdot \left(\frac{\sigma_c(\lambda)}{\sigma_t(\lambda)} - 1 \right) \cdot c_c(t) = \alpha(0, \lambda) \cdot \left(\frac{\sigma_t(\lambda)}{\sigma_c(\lambda)} - 1 \right) \cdot c_t(t) \quad (15)$$

Then, considering Equation (9), by fitting the time evolution to the photoequilibrium of $\Delta\alpha$ at specific wavelengths makes it possible to determine the parameters, τ and $c_c(\infty)$ (or $c_t(\infty)$), needed to calculate the photoisomerization quantum yields, according to Equation (13).

From Equation (15), it is worth noting that isosbestic points ($\Delta\alpha = 0$) occur at wavelengths for which $\sigma_t = \sigma_c$.

2.2. Absorption Spectral Properties

The extinction coefficient spectra of all-trans- and 13-cis-CR in methanol (MeOH) and aqueous solutions are reported in Figure 3A. In MeOH, the all-trans isomer was characterized by the main peaks at 432 and 458 nm and a shoulder at around 409 nm. The 13-cis isomer presented visible bands slightly shifted at lower wavelengths, 426 and 452 nm, and a marked band at 320 nm. The extinction coefficient (ϵ) of 13-cis-CR at the main peak was about 30% lower than the all-trans-CR, at $64.7 \text{ kM}^{-1} \text{ cm}^{-1}$ versus $89.7 \text{ kM}^{-1} \text{ cm}^{-1}$.

In H_2O , the main peaks occurred at 442 ($\epsilon = 85.7 \text{ kM}^{-1} \text{ cm}^{-1}$) and 432 nm ($\epsilon = 51.3 \text{ kM}^{-1} \text{ cm}^{-1}$) for all-trans-CR and 13-cis-CR, respectively, slightly shifted towards longer wavelengths with respect to the methanolic solution. The “cis” peak was present at 326 nm.

2.3. Direct Photoisomerization

Because of the above absorption properties of isomers, the photon-induced conversion of all-trans-CR to 13-cis-CR determined the typical difference absorbance (DA) spectrum (irradiated minus unirradiated) depicted in Figure 3B,C, with negative bands in the visible and a positive band in the UV spectral region. Photoisomerization starting from 13-cis-CR produced difference absorbance spectra specular in shape to those starting from all-trans-CR (Figure 3B,C). The reported spectra were obtained after the photoequilibrium was reached.

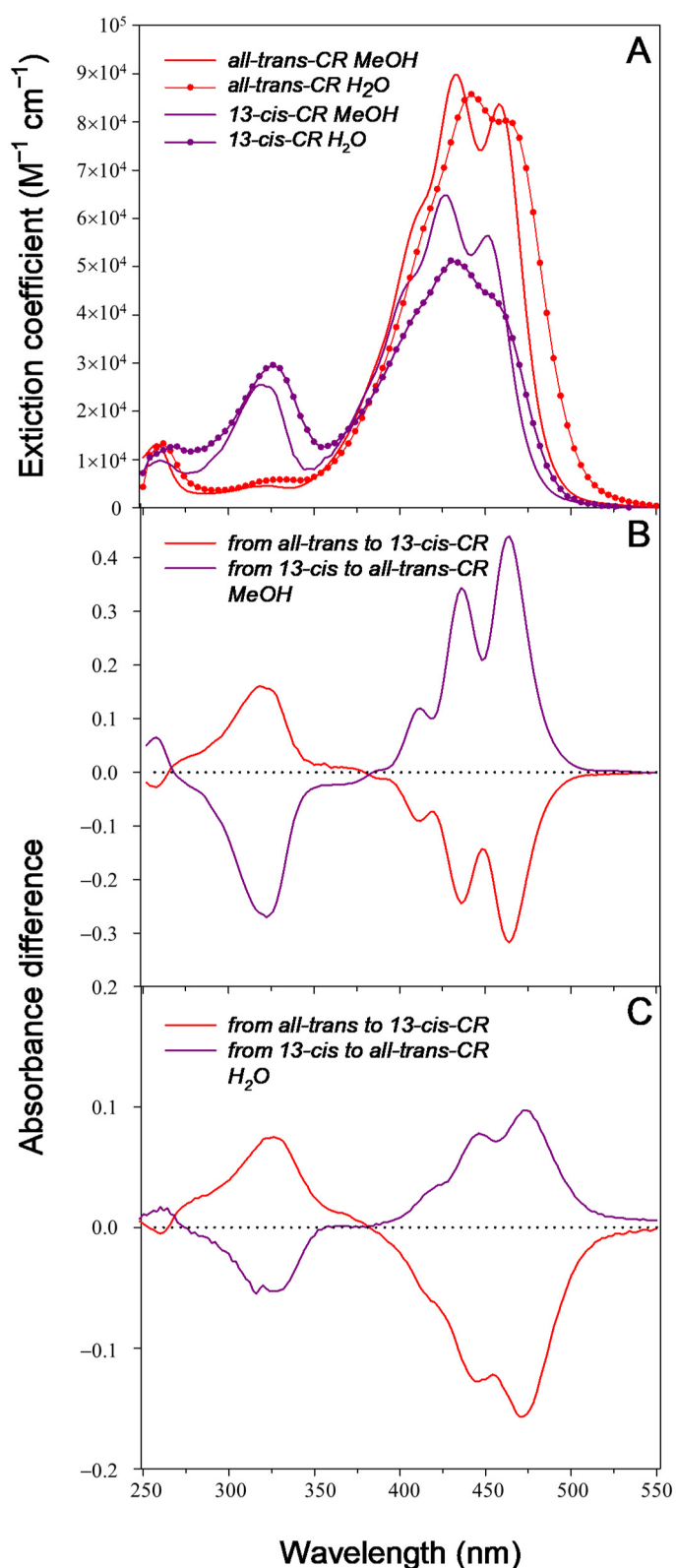


Figure 3. Extinction coefficients of all-trans-CR and 13-cis-CR in methanol and water (A). Difference (irradiated minus unirradiated) absorbance spectra recorded after irradiation at 488 nm to the photoequilibrium of both solutions of all-trans- (dashed red line) and 13-cis-CR (purple line) in methanol (B) and water (C) on a 1 cm pathlength. The initial concentration was 15 μM and 5 μM for all-trans- and 13-cis-CR solutions, respectively.

Both spectra showed isosbestic points at 266 and 380 nm. Variation of absorbance at these wavelengths could be used to check if some other products or bleaching of the molecules occurred. The wavelengths of maximal molar extinction difference at 321 and 463 nm could instead be used to follow the change of 13-cis-CR and all-trans-CR concentrations starting from pure compound solutions.

Figure 4 shows the time evolution of the DA spectra peak values at 321 and 463 nm of methanolic solutions, both aerated (saturated with molecular oxygen) or deoxygenated (by argon bubbling), exposed to a constant photon fluence rate at 488 nm, starting from all-trans-CR. The two peaks changed in opposite direction, indicating the formation of 13-cis-CR and the disappearance of the all-trans isomer.

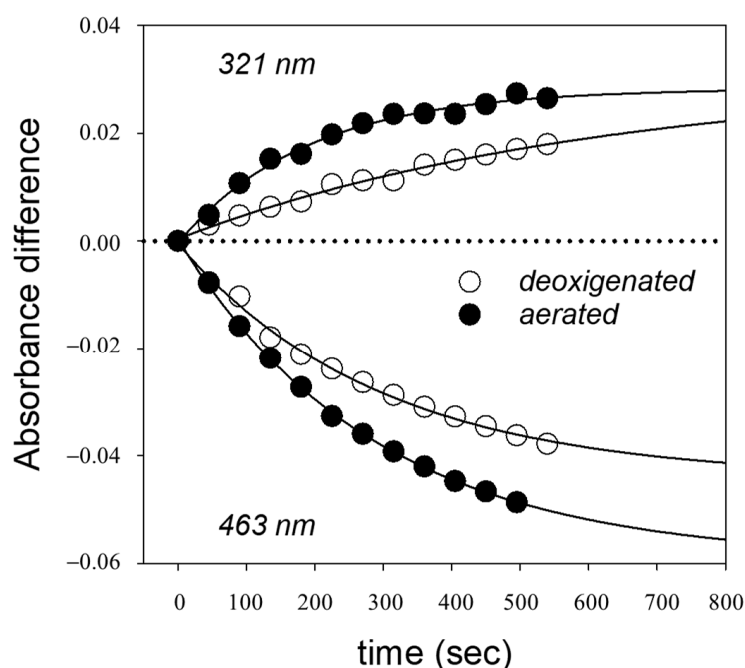


Figure 4. Time evolution of the difference absorbance values at 321 and 463 nm during irradiation at 488 nm, starting from a solution of all-trans-CR in methanol at the concentration of 7.25 μM . Full line represents the data-fitting exponential curves.

The experimental data of Figure 4 were accurately fitted by an exponential curve. Hence, the formation of the 13-cis isomer followed a first-order kinetics up to a photoequilibrium. Analogously, the time evolution of difference absorbances during photoisomerization starting from the 13-cis-CR are reported in Figure S1.

The presence of oxygen did not appreciably affect the spectral values at the isosbestic points; consequently, no reaction of photooxidation was observed. Furthermore, the photoisomerization reaction was faster in the presence of oxygen than without oxygen.

According to Equation (15), the 13-cis-CR concentration at any time t was proportional to the DA and could be evaluated once the $\sigma_{\text{cis}}/\sigma_{\text{trans}}$ ratio was known.

The quantum yields of photoisomerization evaluated by using Equation (13) for irradiated solutions of all-trans- ($\phi_{c,m}$) or 13-cis-CR ($\phi_{t,m}$), defined as directly measured, are reported in Table 1. These values were then used in Equation (12) to predict the quantum yields of the back reactions, cis to trans ($\phi_{t,p}$) and trans to cis ($\phi_{c,p}$), respectively, by the model used to describe the kinetics of CR photoisomers. The comparison between directly measured (m) and predicted (p) quantum yields is useful to check the accuracy of the photoisomerization model.

Table 1. Average values (\pm SD) of quantum yields of trans \leftrightarrow cis photoisomerization and 13-cis-CR photoequilibrium concentration under laser irradiation at 488 nm.

	$\phi_{c,m}$	Trans \rightarrow Cis $\phi_{c,p}$ (Predicted by Equation (12))	$C_c(\infty)$ (%)	$\phi_{t,m}$	Cis \rightarrow Trans $\phi_{t,p}$ (Predicted by Equation (12))	$C_c(\infty)$ (%)
MeOH Argon saturated	$4.75 \pm 2.10 \times 10^{-4}$	$3.14 \pm 1.23 \times 10^{-4}$	17.6 ± 1.7	$2.10 \pm 0.76 \times 10^{-3}$	$6.31 \pm 2.71 \times 10^{-3}$	30.8 ± 9.7
MeOH Oxygen saturated	$1.11 \pm 0.37 \times 10^{-3}$	$1.65 \pm 0.62 \times 10^{-3}$	19.3 ± 2.5	$1.16 \pm 0.29 \times 10^{-2}$	$1.30 \pm 0.26 \times 10^{-2}$	29.4 ± 11.9
H ₂ O Argon saturated	$2.6 \pm 0.6 \times 10^{-4}$	$1.8 \pm 0.7 \times 10^{-4}$	17.0 ± 2.8	$2.4 \pm 0.4 \times 10^{-3}$	$6.2 \pm 1.4 \times 10^{-3}$	26.2 ± 4.1

These calculations were performed by using the DA values at both the 463 and 321 nm. Although there was a tendency to obtain higher values of quantum yields by following the cis peak at 321 nm, no significant difference between the average values calculated at the two spectral bands ($p > 0.5$, according to Welch's *t*-test) was observed. Consequently, we grouped the two data sets, and report the resulting average values in Table 1. In the same Table, the photoequilibrium concentration of 13-cis-CR determined by the spectrophotometric analysis is reported.

In Ar-saturated MeOH solutions, the $\phi_{c,m}$ in the trans \rightarrow cis photoisomerization was 4.4-times lower than $\phi_{t,m}$ in the cis \rightarrow trans photoreaction. In addition, $\phi_{c,m}$ was more than one order of magnitude (13.3 times) lower than $\phi_{t,p}$, as predicted by the photoisomerization model. Starting from the 13-cis-CR (cis \rightarrow trans) still produced higher values for the measured $\phi_{t,m}$ than the predicted $\phi_{c,p}$ ($\frac{\phi_{t,m}}{\phi_{c,p}}$ ratio = 6.7).

On the other hand, the $\phi_{c,m}$ directly measured was significantly ($p = 0.038$) higher than that predicted by Equation (12) starting from the 13-cis-CR ($\phi_{c,p}$) and the $\phi_{t,m}$ measured was three times lower than that predicted ($\phi_{t,p}$) ($p < 0.001$).

In oxygen-saturated MeOH solutions, both cis and trans quantum yields were higher than those in Ar-saturated solutions, 2.3 and 5.5 for the measured $\phi_{c,m}$ and $\phi_{t,m}$, respectively. The presence of oxygen, therefore, favored the photoisomerization of crocins.

For both solutions, the 13-cis-CR concentration of photoequilibrium starting from 13-cis-CR was higher (52–74%) than that obtained by starting from all-trans-CR.

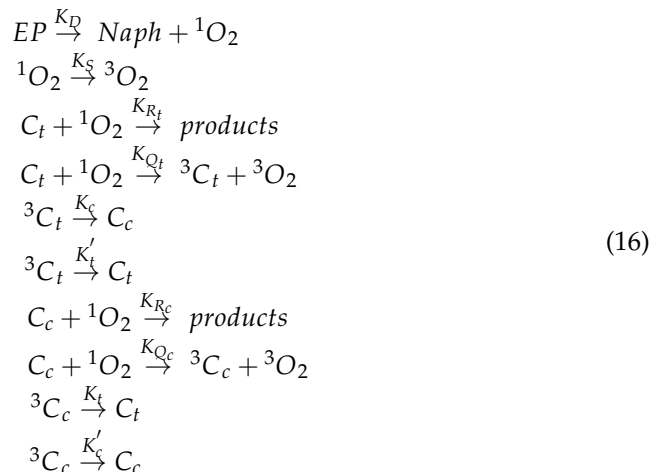
In Ar-saturated water solutions, the measured $\phi_{t,m}$ starting from 13-cis-crocin was one order of magnitude higher than the measured $\phi_{c,m}$ starting from all-trans. The predicted $\phi_{t,p}$ was even much higher (24 times) than the measured $\phi_{c,m}$.

On the other hand, the directly measured $\phi_{c,m}$ was not significantly ($p = 0.187$) different than that predicted by Equation (12) starting from the 13-cis-CR, while the measured $\phi_{t,m}$ was significantly ($p = 0.036$) lower than that predicted ($p < 0.001$).

The 13-cis-CR concentration of photoequilibrium starting from 13-cis-CR was 1.5-times higher than that obtained by starting from all-trans-CR.

2.4. Kinetics of the CR-¹O₂ Reactions

All of the processes occurring during the reactions between CR and ¹O₂ (Figure 2) can be described by the following Equations.



where EP is the endoperoxide that produces the naphthalenic acid (Naph) and ¹O₂ with the thermal dissociation rate *K_D* (see Materials and Methods section); *C_t* and *C_c* represent the concentration of all-trans- and 13-cis-CR in the stationary state (or triplet state: ³*C_t* and ³*C_c*). *K_{Q_{t,c}}* and *K_{R_{t,c}}* are the bimolecular rate constants for physical and chemical quenching of ¹O₂, respectively. The deexcitation rates of the CR triplet states are indicated by *K_t* and *K_c* for the trans↔cis isomerization processes and by *K'_t* and *K'_c* for the internal relaxation processes. The rate constants for the natural decay of ¹O₂, *K_S*, was determined to be 1.43 × 10⁵ s⁻¹ in MeOH [36] and 2.4 × 10⁵ s⁻¹ [36] in H₂O [37].

The time evolution of concentrations is given by

$$\begin{aligned}
 \dot{C}_t &= K'_t {}^3C_t + K_t {}^3C_c - (K_{Q_t} + K_{R_t}) C_t {}^1\text{O}_2 \\
 \dot{C}_c &= K'_c {}^3C_c + K_c {}^3C_t - (K_{Q_c} + K_{R_c}) C_c {}^1\text{O}_2 \\
 \dot{{}^3C}_t &= K_{Q_t} C_t {}^1\text{O}_2 - (K_c + K'_t) {}^3C_t \\
 \dot{{}^3C}_c &= K_{Q_c} C_c {}^1\text{O}_2 - (K_t + K'_c) {}^3C_c \\
 \dot{{}^1\text{O}}_2 &= K_D EP Y_{SO} - [K_S + (K_{Q_t} + K_{R_t}) C_t + (K_{Q_c} + K_{R_c}) C_c] {}^1\text{O}_2
 \end{aligned} \tag{17}$$

Within the steady-state approximation, ³ $\dot{C}_t = \dot{{}^3C}_c = 0$, we have that

$${}^3C_t = \frac{K_{Q_t} C_t {}^1\text{O}_2}{K_c + K'_t}; \quad {}^3C_c = \frac{K_{Q_c} C_c {}^1\text{O}_2}{K_t + K'_c} \tag{18}$$

that combined with Equation (17) lead to

$$\begin{aligned}
 \dot{C}_t &= [-(Y_c K_{Q_t} + K_{R_t}) C_t + Y_t K_{Q_c} C_c] {}^1\text{O}_2 \\
 \dot{C}_c &= [-(Y_t K_{Q_c} + K_{R_c}) C_c + Y_c K_{Q_t} C_t] {}^1\text{O}_2
 \end{aligned} \tag{19}$$

with

$$Y_c = \frac{K_c}{K_c + K'_t}; \quad Y_t = \frac{K_t}{K_t + K'_c} \tag{20}$$

as defined above in the photoisomerization section (Equation (6)).

At the initial stage of the C_t-¹O₂ reaction, around t = 0, from the last of Equation (17) we have that

$${}^1\text{O}_2 = \frac{K_D EP_0 Y_{SO}}{K_S + (K_{Q_t} + K_{R_t}) C_{t0}} \tag{21}$$

that used in Equation (19) allows to calculate

$$Y_c = -\dot{C}_{t0} \cdot \frac{K_s + (K_{Q_t} + K_{R_t})C_{t0}}{K_{Q_t}C_{t0} \cdot K_D EP_0 Y_{SO}} - \frac{K_{R_t}}{K_{Q_t}} \quad (22)$$

Analogously, for the $C_c^{-1}O_2$ reaction we obtain

$$Y_t = -\dot{C}_{c0} \cdot \frac{K_s + (K_{Q_c} + K_{R_c})C_{c0}}{K_{Q_c}C_{c0} \cdot K_D EP_0 Y_{SO}} - \frac{K_{R_c}}{K_{Q_c}} \quad (23)$$

At the steady state, being $\dot{C}_t = \dot{C}_c = 0$, Equation (19) gives

$$\begin{aligned} (Y_c K_{Q_t} + K_{R_t})[C_t]_{\infty} &= Y_t K_{Q_c} [C_c]_{\infty} \\ (Y_t K_{Q_c} + K_{R_c})[C_c]_{\infty} &= Y_c K_{Q_t} [C_t]_{\infty} \end{aligned} \quad (24)$$

2.5. Singlet-Oxygen-Induced CR Isomerization

2.5.1. Methanolic Solutions

In the reaction between crocin and singlet oxygen generated by the thermal dissociation of the 1,4-endoperoxide of 3-(4-methyl-1-naphthyl)propionic acid (EP) in MeOH, we observed difference absorbance spectra, determined as absorbance at time t of the reaction at 35 °C minus the absorbance at time 0, rather similar to those obtained by irradiation (Figure 5). The spectra were corrected for the EP absorption spectrum (Figure S2A of the Supplementary Materials) that partially overlaps to the CR absorbance spectra in the UV range. Difference absorbance at the isosbestic point (around 380 nm) remained constant during the reaction, indicating that bleaching reactions were negligible during the measuring time adopted.

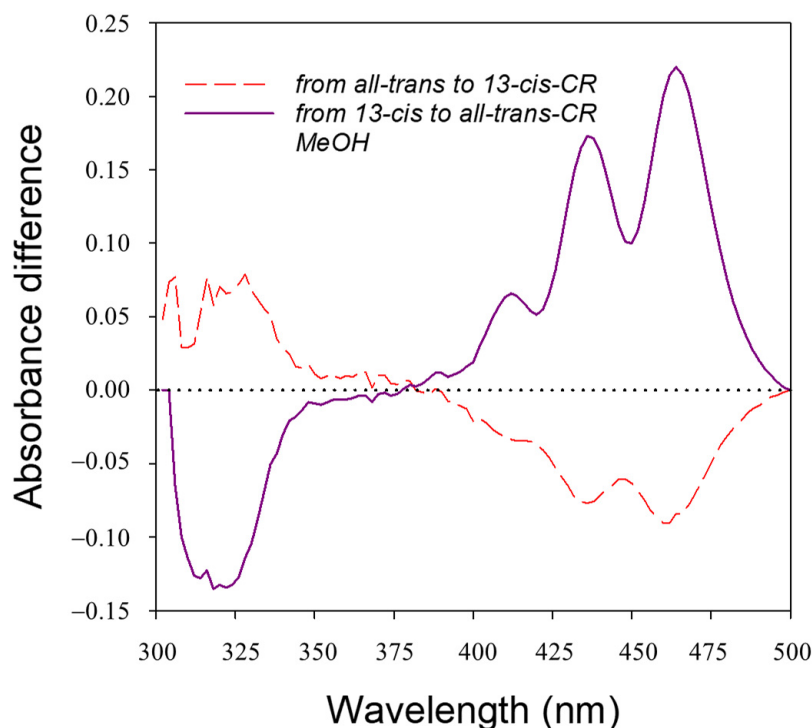


Figure 5. Difference absorbance spectra between a methanolic solution of CR and EP after 30' of reaction at 35 °C with respect to the time 0 solution, starting from all-trans- (dashed red line) and 13-cis-CR (purple line) solutions, both with an initial concentration of 10.5 μ M.

As in the case of photoisomerization, the *all-trans* \leftrightarrow *cis* conversion could be followed by the change in the DA at the maximal molar extinction difference at 463 nm. Using the

second peak of the DA at 321 nm is more difficult because of the partial overlapping of the EP absorption. Simultaneous measurement of the absorbance at 266 nm (see evolution in Figure S2B) was used to calculate the release of $^1\text{O}_2$ that appeared almost linear with time, even if the best fit of data required an exponential function.

Figure 6 shows the time evolution of the DA spectra peak values at 463 nm of methanolic solutions during the reaction with $^1\text{O}_2$ of both all-trans- and 13-cis-CR.

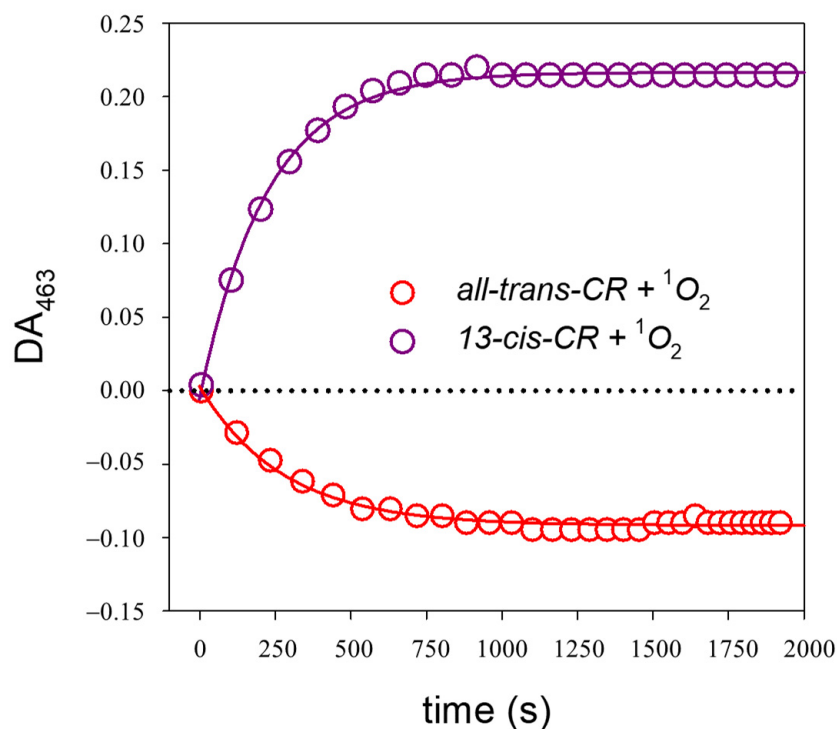


Figure 6. Time evolution of the difference absorbance values at 463 nm during the reaction of CR with $^1\text{O}_2$, starting from a solution of all-trans-CR (red line) or 13-cis-CR (purple line) in methanol, both at the concentration of 10.5 μM . Full line represents the data-fitting exponential curves.

Because of the absence of significant bleaching, Equations (22) and (23) modify as follows:

$$Y_c = -\dot{C}_{t0} \cdot \frac{K_s + K_{Q_t} C_{t0}}{K_{Q_t} C_{t0} \cdot K_D EP_0 Y_{SO}} \quad (25)$$

$$Y_t = -\dot{C}_{c0} \cdot \frac{K_s + K_{Q_c} C_{c0}}{K_{Q_c} C_{c0} \cdot K_D EP_0 Y_{SO}} \quad (26)$$

The rate constants of the $^1\text{O}_2$ physical quenching in MeOH were previously determined by the Young's method [38] and were $K_{Q_t} = 7.37 \times 10^9 \text{ M}^{-1} \text{ s}^{-1}$ and $K_{Q_c} = 6.46 \times 10^9 \text{ M}^{-1} \text{ s}^{-1}$ for all-trans- and 13-cis-CR, respectively (Speranza, personal communication).

By measuring the initial CR conversion rate from the exponential curve fitting of the kinetics of the DA_{463} (Figure 6) and the initial EP concentration, we could calculate the relative yields of isomerization from the triplet state.

These data for both the *all-trans* \rightarrow *cis* (Y_c) and the *cis* \rightarrow *all-trans* (Y_t) reactions are reported in Table 2, as measured (m) and predicted (p) values.

Table 2. Average values (\pm SD) of yields of *all-trans* \leftrightarrow *cis* isomerization and 13-*cis*-CR equilibrium concentration induced by the reaction with singlet oxygen.

	$Y_{c,m}$	<i>all-trans</i> \rightarrow <i>cis</i> $Y_{c,p}$ Predicted	$C_c(\infty)$ (%)	$Y_{t,m}$	<i>cis</i> \rightarrow <i>all-trans</i> $Y_{t,p}$ Predicted	$C_c(\infty)$ (%)
MeOH	0.113 ± 0.009	$0.180 \pm 0.038^*$	20.5 ± 0.3	0.215 ± 0.031	$0.501 \pm 0.048^*$	48.7 ± 2.0
H ₂ O	0.058 ± 0.009	$0.115 \pm 0.017^{**}$	13.9 ± 1.3	0.318 ± 0.048	$0.1650 \pm 0.073^{**}$	23.0 ± 4.0

* From Equation (27); ** From Equation (24).

The $Y_{c,m}$ was about half the yield measured for all-*trans* isomerization starting from 13-*cis*-CR.

Following the reaction until the steady state, the equilibrium relative concentration of 13-*cis*-CR starting from all-*trans* was calculated to be about 20% (Table 2). At this stage, $\dot{C}_t = 0$, and the Equation (24), with K_{R_t} and K_{R_c} negligible, give

$$Y_c K_{Q_t} C_{t\infty} = Y_t K_{Q_c} C_{c\infty} \quad (27)$$

that makes it possible to predict the yields Y_t for the back isomerization to be almost five times higher than the measured $Y_{c,m}$ (Table 2).

The 13-*cis*-CR concentration of equilibrium was more than double starting from 13-*cis*-CR with respect to that obtained by starting from all-*trans*-CR, while the predicted $Y_{c,p}$ was not significantly different than the measured $Y_{c,m}$.

2.5.2. Aqueous Solutions

The analysis of the ¹O₂-induced isomerization of crocin in water solutions is complex because of the presence of non-negligible bleaching reactions. This process was evidenced by the HPLC data of samples processed at different times of the reaction.

In Figure 7A, the decrease with time in the total HPLC area of compounds detected for both the all-*trans*- and 13-*cis*-CR reactions with ¹O₂ is reported, as an index of the bleaching of compounds. However, at the same time, the process of isomerization still occurred, as recognized by the kinetics of the relative isomer concentrations shown in Figure 7B,C for the all-*trans* to *cis* and the *cis* to all-*trans* conversions, respectively.

As in the case of the MeOH solutions, to calculate the isomerization yields from Equations (22) and (23), we need to know the chemical and physical ¹O₂-quenching rate constants for the two crocin isomers in the aqueous medium. The rate constants, K_{Q_t} and K_{R_t} , for the all-*trans*-CR were previously reported [23]; however, the reaction model considered in that study was not complete since the all-*trans* to 13-*cis* isomerization was neglected.

On the other hand, the chemical bleaching reaction was considered to occur when starting from all-*trans*-CR but not when starting from 13-*cis*-CR.

We have the evidence that both bleaching and isomerization processes are present whatever the starting reaction CR isomer is and, therefore, the rate constant values previously reported must be revised.

Our HPLC analysis of the reactions made it possible to determine the rate of compound disappearance by fitting the change with time of the total chromatograph peak areas (Figure 7A), as well as the rate of isomerization by fitting the change with time of the isomer-relative concentrations (Figure 7B,C).

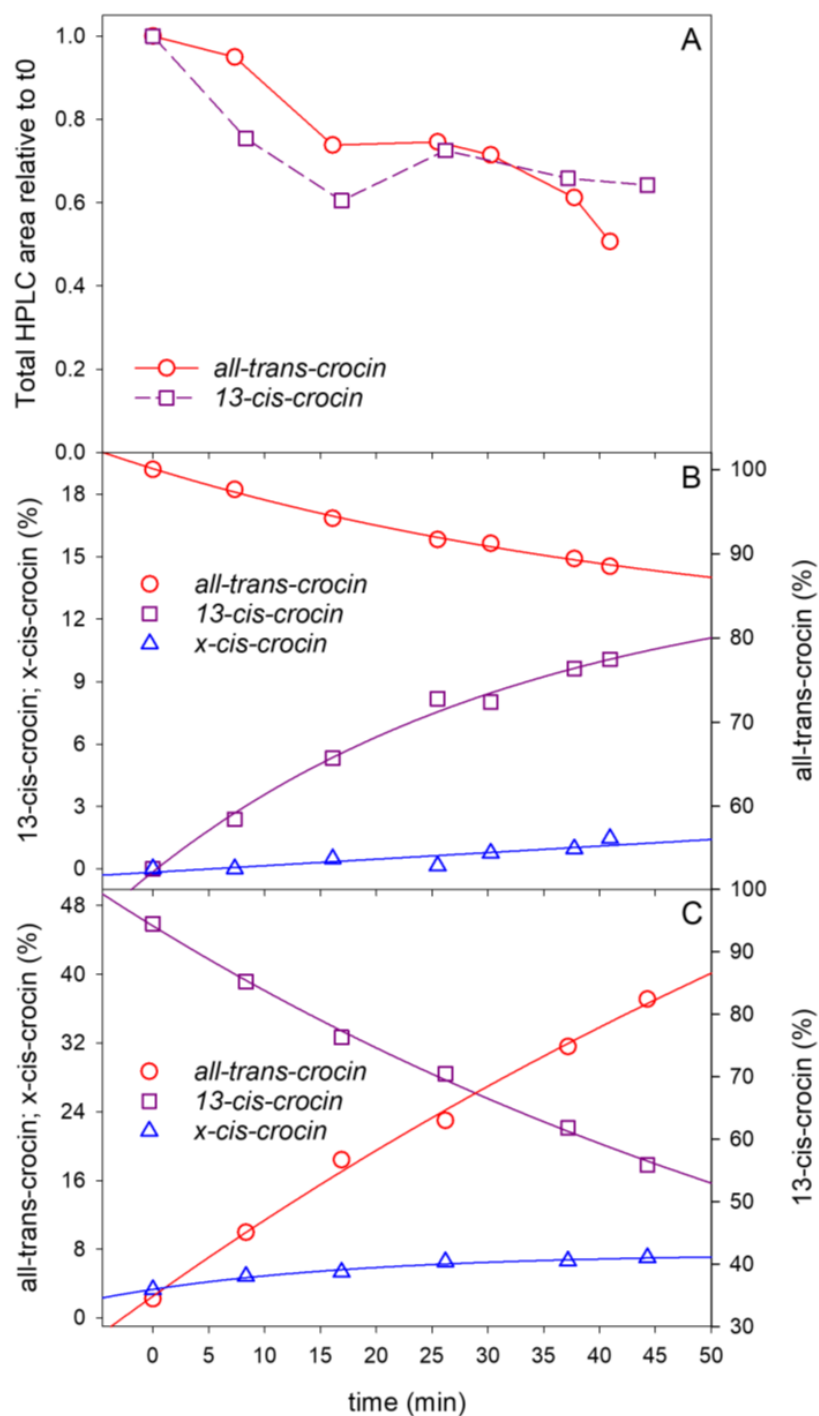


Figure 7. Variation of the total HPLC area of crocin compounds with time of their reaction with $^1\text{O}_2$ (A). Kinetics of the relative concentration of crocin isomers induced by the reaction with $^1\text{O}_2$ starting from all-trans-crocin (B) or from 13-cis-crocin (C). The solid lines in B and C represent the exponential function fitting of data.

As a result, for the all-trans-CR reaction with $^1\text{O}_2$, the isomerization rate ($Y_c K_{Q_t}$) was 1/3 of the rate of bleaching (K_{R_t}), leading to the recalculated rate constants as

$$K_{R_t} = 0.42 \cdot 10^8 \text{ M}^{-1}\text{s}^{-1} \text{ and } K_{Q_t} = 1.81 \cdot 10^9 \text{ M}^{-1}\text{s}^{-1}$$

For the 13-cis-crocin reaction with $^1\text{O}_2$, assuming a rate of bleaching (K_{R_c}) similar to that calculated for all-trans-CR, the resulting physical quenching rate constant was

$$K_{Q_c} = 1.85 \cdot 10^9 \text{ M}^{-1}\text{s}^{-1}$$

According to the revised rate constants, we calculated the relative yields of isomerization from the triplet state for both the all-trans \rightarrow cis (Y_c) and the cis \rightarrow all-trans (Y_t) reactions, as reported in Table 2.

The Y_c was 5.5 times lower than the yield measured for all-trans isomerization starting from 13-cis-CR and about one order of magnitude lower than the Y_t predicted by the model (Equation (24)).

The measured Y_c was also significantly ($p = 0.002$) lower than the predicted Y_c starting from 13-cis-CR.

The 13-cis-CR concentration of equilibrium was significantly ($p = 0.048$) higher starting from 13-cis-crocin with respect to that obtained by starting from all-trans-crocin.

Following the $^1\text{O}_2$ -CR reaction by the HPLC analysis, it is evident that a third compound, called x-cis-CR, appeared and increased with time (Figure 7). Its amount was limited to about 1.5% of the total compounds when the reaction was started from all-trans (Figure 7B), while it reached about 7% in the 13-cis-CR reaction with $^1\text{O}_2$ (Figure 7C).

3. Discussion

In this work, we performed a complete analysis of the photon and $^1\text{O}_2$ induction of the cis–trans isomerization in the water-soluble carotenoid CR. The proposed spectrophotometric method allowed the simultaneous monitoring of the configurational change, possible bleaching and the $^1\text{O}_2$ production during the whole process.

Photoisomerization was followed at two absorption bands, that is, one close to the second main peak of absorption (463 nm) and the other at the “cis” absorption peak (321 nm). During the photoisomerization, absorbance at these two bands changed in an opposite direction and depending on the starting molecule (Figures 3, 4 and S1). The process was reversible and concerned essentially only two isomers, the all-trans- and 13-cis-CR, as proved by the presence of an isosbestic point in the DA spectra, without any significant bleaching. If other cis isomers were involved, they should have been produced at rather low amounts and should have had absorption properties similar to the 13-cis-CR.

The presence of the single 13-cis-isomer means that this is the most stable configuration with the highest rotational energy barrier to switch to all-trans. The other possible cis isomers are not formed at significant amounts or are rapidly isomerized back to all-trans because of lower rotational barriers, to be confirmed with theoretical studies similar to those applied to β -carotene and lycopene cis–trans isomerization [39].

Interestingly, results in term of isomerization quantum yields and isomer photoequilibrium concentrations obtained in both water and methanolic solutions were rather similar, and closely recall that described for β -carotene in non-polar solvents [16,18,19].

It is likely that the cis–trans isomerization occurs as relaxation of the CR triplet excited state through a twisted intermediate state common to the all-trans and 13-cis isomers.

The much larger (>10 -times) ϕ_t with respect to ϕ_c suggests the presence of a higher rotational energy barrier from the all-trans triplet state than from the 13-cis-CR, analogously to the triplet potential energies calculated for β -carotene and lycopene [39].

The involvement of the carotenoid triplet state in the isomerization process is confirmed by the photoisomerization results obtained in the methanolic solution saturated with molecular oxygen (Table 1). In fact, oxygen is known to induce inter-system crossing [40] that enhances ϕ_c and ϕ_t by about 2- and 5-fold, respectively, with respect to those in argon-saturated solutions, without appreciable bleaching.

No data about the quantum yield for photoisomerization of crocinoids are reported in the literature. However, Craw and Lambert [33] indicated a quantum yield of triplet formation of crocetin of less than 10^{-3} in oxygen-free aqueous solutions. This is due to the competition between the internal conversion and intersystem crossing in the singlet excited-

state relaxation process, in favor of the internal conversion. Accordingly, our value of ϕ_c that is about an order of magnitude lower (Table 1), is consistent with a photoisomerization pathway involving the excited triplet state.

Analyzing the CR- $^1\text{O}_2$ interaction in methanolic solutions, we still observed the all-trans \leftrightarrow cis reversible conversion with spectral absorbance changes similar to those generated by photoisomerization (Figures 5 and 6). In water solutions, however, a certain amount of compound bleaching appeared along with the isomerization process.

It is generally accepted that physical quenching is the primary way carotenoids reduce singlet oxygen [11]. As depicted in Figure 2, once a CR isomer reaches its triplet state, produced by the energy transfer from $^1\text{O}_2$, it can decay back to the starting configuration or rotate around the C13=C14 double bond, leading to the twisted configuration. The measured yield of cis \rightarrow all-trans isomerization from the triplet state, $Y_{t,m}$, was about 1.9 (MeOH) and 5.5 (H₂O) times higher than $Y_{c,m}$, confirming again the easier pathway for the cis to trans rotation with respect to the opposite, analogously to what happens in the photoisomerization.

In MeOH solutions, we did not observe any significant bleaching occurring during the CR- $^1\text{O}_2$ reaction. This is in accordance with the literature, showing that the $^1\text{O}_2$ chemical quenching by carotenoids occurs to a much lower extent with respect to physical quenching [3,22,24]. Even in a reverse micelle system, used to study the medium heterogeneity effect on the $^1\text{O}_2$ quenching rate constants, K_Q for different carotenoids was about four orders of magnitude higher than K_R [27].

In the characterization of the CR isomerization, it is also essential to compare the $^1\text{O}_2$ -quenching ability of the cis and trans isomers. The rate constants of the $^1\text{O}_2$ physical quenching in organic solvents for both CR isomers were found to be lower than those of all-trans- and cis- β -carotene, in accordance with their lower number of conjugated double bonds [15]. The difference in K_Q between all-trans- and 13-cis-CR was around 15%, as was observed between all-trans and 15-cis- β -carotene [15]. Accordingly, in aqueous solutions, we estimated quite similar values of K_{Q_t} and K_{Q_c} .

Some authors [41,42] have suggested that the cis geometrical configurations of astaxanthin possess higher antioxidant properties with respect to the all-trans configuration. Although a clear mechanism for that has not been found yet, it is possible that this difference is related to the more efficient isomerization from cis to all-trans than vice versa, as we observed in the CR- $^1\text{O}_2$ reaction, that can promptly quench ROS without any significant chemical consumption of molecules.

For CR in H₂O, we found that for both isomers, K_Q was at least 40 times higher than K_R . However, in this medium, the disappearance of the starting compound was not negligible (Figure 7A).

The photon- and $^1\text{O}_2$ -induced-reactions model we used properly described the isomerization processes from all-trans- to 13-cis-CR. However, when starting the reactions from the 13-cis isomer, some discrepancies in terms of absolute values of quantum yields, triplet state decay yields and relative concentrations of isomers with respect to the process starting from all-trans-CR were found.

We do not have a conclusive explanation for that. The observed inconsistency can be due to the limited purity of the starting 13-cis solutions and/or to the involvement in the isomerization processes of more than the two all-trans and 13-cis compounds. Indeed, in the H₂O medium, clear evidence of the $^1\text{O}_2$ -induced production of an additional molecule was reported (Figure 7C). It could not be definitely identified; however, it is likely to be another cis or a di-cis-isomer of CR.

This explanation should be in accordance with the isomerization patterns and quantum yields proposed by Kuki et al. [16] for the triplet-sensitized and direct photoisomerization of β -carotene. In synthesis, the trans to cis isomerization is mainly favored towards the central cis-isomers; the cis to all-trans isomerization is the far more efficient process for the central cis-isomers but with significant chances to produce other cis- or di-cis-isomers.

4. Materials and Methods

4.1. Chemicals and Solutions

Crocin was extracted and purified from commercially available saffron according to Speranza et al. [35]. The isolation of the all-trans and 13-cis configurational isomers was achieved by preparative HPLC [35]. Di-n-octylamine for HPLC was from Aldrich-Chemie, Germany, and other chemicals were analytical- or HPLC-grade reagents. Phosphate buffer solutions were purged with Ar.

The spectral extinction coefficients of all-trans-CR (ϵ_t) in both methanolic and aqueous solutions were measured directly. For 13-cis-crocin, since its HPLC analysis showed the content of about 20% of unidentified impurities, the ϵ_c spectrum was indirectly estimated from the difference absorbance spectrum of an all-trans-CR solution irradiated to the photoequilibrium and measuring the $C_c(\infty)$ and $C_t(\infty)$ isomer concentrations by HPLC.

Solutions of *all-trans*- and *13-cis*-CR were prepared by dissolving small amounts of the pigment (0.3–0.5 mg) directly in methanol or 0.1 M sodium phosphate buffer (pH 7.4). They were either deoxygenated by Ar bubbling or aerated (saturated by O₂ bubbling).

Fresh crocin solutions were prepared each day and manipulated under dim red light.

4.2. Monitoring of Photoreactions

Samples of CR solutions (volume 0.44 mL), with concentrations ranging from 5 μ M to 15 μ M, were irradiated (argon laser, in the cell compartment of a spectrophotometer (PYE UNICAM model 8800) at the 488 nm Ar laser (Spectra-Physics model 165-008) line. An unirradiated sample was maintained in the reference position in order to record differential absorption values. Variations of the differential absorbance during irradiation were simultaneously monitored at 321, 463 and 380 nm, corresponding respectively to the negative and positive maximum and to the isosbestic point of the differential absorption spectrum of the *all-trans*/*13-cis* CR mixture. The 380 nm wavelength was an isosbestic point, so that its variation could be considered an index of the presence of photobleaching or the photoproduction of other compounds in addition to *all-trans*- and *13-cis*-CR. A 2 \times 10 mm quartz cuvette was used, with the thinner side exposed to the laser light to minimize light attenuation across the solution. The laser beam was expanded to provide essentially uniform energy irradiance across the cuvette face.

The photon fluence rate at the cuvette surface was about $F = 1.9 \times 10^{16}$ photons $\text{cm}^{-2} \text{s}^{-1}$ (laser power meter: EG&G model 460, instrumental accuracy = 5%). Measurements were carried out at 26 ± 2 °C.

4.3. Singlet Oxygen Production and Reaction Monitoring

Singlet molecular oxygen was produced by the thermal dissociation of 3-(1,4-epidioxy-4-methyl-1,4-dihydro-1-naphthyl)propionic acid (EP) to produce naphthalenic acid (Naph).

The ¹O₂ concentration with time could be determined by measuring the evolution of the Naph concentration corrected for the yield of ¹O₂ formation, Y_{SO} , that was earlier estimated to be more than 82% in methanol [43] and 45% in H₂O [44].

The Naph concentration was measured spectrophotometrically by the absorbance at 266 nm (isosbestic point for the *all-trans*- \leftrightarrow -*cis*-CR isomerization) according to an exponential function defined as

$$A_{Naph}^{266}(t) = \epsilon_{Naph}^{266} [EP]_0 (1 - e^{-K_D t}) \quad (28)$$

where ϵ_{Naph}^{266} is the molar extinction coefficient of Naph at 266 nm, $[EP]_0$ is the initial concentration of the endoperoxide, K_D is the decomposition rate constant of the endoperoxide. This method was previously used to calculate the ¹O₂-quenching rate constants of anthracylines, bixinoids and crocinoids [23,25,37]. It is advantageous with respect to photochemical ¹O₂ production since it avoids the direct *cis*-*trans* photoisomerization of carotenoids.

Two separate solutions of crocin (about 15 μ M) and EP (about 5 mM) in methanol or phosphate buffer were mixed at 0 °C. At this temperature the decomposition of EP to

Naph is negligible [43]. The resulting solution was deoxygenated by Ar bubbling and then rapidly heated to 35 °C by a Peltier device and maintained at this temperature (± 0.1 °C) inside the spectrophotometer.

The time evolution of the CR- $^1\text{O}_2$ reaction was monitored following the temporal changes of the absorbance at 463 nm, the maximum of the isomerization difference absorption spectrum. The bleaching of crocin was simultaneously checked by measuring absorbance at 380 nm, isobestic point between the two crocin isomers. The overlapping of the Naph absorbance with that of the cis/trans-CR mixture in the ultraviolet region below 340 nm made it impossible to follow the evolution of the “cis peak” at 321 nm.

4.4. HPLC Analysis

Crocin solutions were analyzed by an isocratic reversed-phase HPLC using a Waters Liquid Chromatograph fitted with a model 740 integrator, a 5 μm , 25 \times 0.46 cm Ultrasphere ODS column (Beckman, CA, USA) or Ultremex ODS column (Phenomenex, Torrance, CA, USA) and a 4.6 \times 0.45 cm precolumn. The eluent was a mixture of water and 0.1 M di-*n*-octylamine acetate in MeOH (1:2 *vol/vol*) at a flow rate of 1 ml min⁻¹.

Before injection, samples (40 mL) from the aqueous solutions were diluted with 0.1 M di-*n*-octylamine acetate in MeOH (80 mL); samples from the MeOH solutions were mixed with one equal volume of H₂O and one of 0.1 M di-*n*-octylamine acetate in MeOH. This precaution avoided undesirable peaks in the chromatograms due to solvent interferences. The mixtures were centrifuged and 50 mL were injected into the column.

Peaks were monitored at 440 nm (absorption maximum) and identified by reference to standards. Cis isomer peak areas were corrected for the difference in the extinction coefficient at 440 nm in the HPLC mobile phase with respect to all-trans (a factor of 1.36).

4.5. Data Analysis

Statistical analysis and curve fitting were carried out with the SigmaPlot for Windows Version 14.0 software (Systat Software, Inc., San Jose, CA, USA). Comparison of mean values was performed according to the Welch's *t*-test, with *p* values < 0.05 considered statistically significant. The coefficient of determination, R², was used to estimate the curve fitting quality.

5. Conclusions

In summary, the present study provides a new insight on the isomerization processes occurring in the water-soluble carotenoid crocin induced by light or by the physical quenching of $^1\text{O}_2$. Although the presence of a significant chemical quenching of $^1\text{O}_2$ in plants was suggested [45], the cis–trans isomerization process can represent an important physiological role in vivo as a tool to quench reactive oxygen species with a limited requirement of regeneration of the carotenoid. Further investigations by time-resolved spectroscopy are needed to better and conclusively characterize the whole isomerization process in the water-soluble crocinoids.

Supplementary Materials: The supporting information can be downloaded at <https://www.mdpi.com/article/10.3390/ijms241310783/s1>.

Author Contributions: Conceptualization, F.F. and G.A.; methodology, F.F. and G.A.; validation, G.R., F.F. and G.A.; formal analysis, G.R., F.F. and G.A.; investigation, F.F., G.S. and G.A.; data curation, F.F.; writing—original draft preparation, G.A.; writing—review and editing, G.R. and F.F.; supervision, G.S.; All authors have read and agreed to the published version of the manuscript.

Funding: This research was funded by Bando Ricerca COVID-19 Toscana, Project SAVES US, by POR-FESR Toscana 2014-2020, Azione 1.1.5.a1), Project EndoLight and by Fondazione CR Firenze, project Device endoscopico per foto-terapia antibatterica intragastrica.

Institutional Review Board Statement: Not applicable.

Informed Consent Statement: Not applicable.

Data Availability Statement: Not applicable.

Conflicts of Interest: The authors declare no conflict of interest.

References

1. Swapnil, P.; Meena, M.; Kumar, S.; Praveen, U. Current Plant Biology Vital roles of carotenoids in plants and humans to deteriorate stress with its structure, biosynthesis, metabolic engineering and functional aspects. *Curr. Plant Biol.* **2021**, *26*, 100203. [[CrossRef](#)]
2. Ben-amotz, A.; Fishler, R. Analysis of carotenoids with emphasis on 9-k p-carotene in vegetables and fruits commonly consumed in Israel. *Food Chem.* **1998**, *62*, 515–520. [[CrossRef](#)]
3. Heymann, T.; Heinz, P.; Glomb, M.A. Lycopene Inhibits the Isomerization of β - Carotene during Quenching of Singlet Oxygen and Free Radicals. *J. Agric. Food Chem.* **2015**, *63*, 3279–3287. [[CrossRef](#)]
4. Khoo, H.; Prasad, K.N.; Kong, K.; Jiang, Y.; Ismail, A. Carotenoids and Their Isomers: Color Pigments in Fruits and Vegetables. *Molecules* **2011**, *16*, 1710–1738. [[CrossRef](#)]
5. Koyama, Y.; Kakitani, Y.; Watanabe, Y. Photophysical properties and light-harvesting and photoprotective functions of carotenoids in bacterial photosynthesis: Structural selections. In *Primary Processes of Photosynthesis, Part 1: Principles and Apparatus*; Renger, G., Ed.; Royal Society of Chemistry: London, UK, 2007; pp. 151–201.
6. Alagoz, Y.; Nayak, P.; Dhami, N.; Cazzonelli, C.I. cis -carotene biosynthesis, evolution and regulation in plants: The emergence of novel signaling metabolites. *Arch. Biochem. Biophys.* **2018**, *654*, 172–184. [[CrossRef](#)] [[PubMed](#)]
7. Shi, J.; Le Maguer, M. Lycopene in Tomatoes : Chemical and Physical Properties Affected by Food Processing Lycopene. *Crit. Rev. Food Sci. Nutr.* **2010**, *40*, 1–42. [[CrossRef](#)]
8. Honda, M.; Takasu, S.; Nakagawa, K.; Tsuda, T. Differences in bioavailability and tissue accumulation efficiency of (all-E)-and (Z)-carotenoids : A comparative study. *Food Chem.* **2021**, *361*, 130119. [[CrossRef](#)]
9. Boileau, T.-M.; Boileau, A.C.; Erdman, E.J., Jr. Bioavailability of all-trans and cis-Isomers of Lycopene. *Exp. Biol. Med.* **2002**, *227*, 914–919. [[CrossRef](#)]
10. Widomska, J.; Kostecka-Guga, A.; Latowski, D.; Gruszecki, I.; Strza, K. Calorimetric studies of the effect of cis -carotenoids on the thermotropic phase behavior of phosphatidylcholine bilayers. *Biophys. Chem.* **2009**, *140*, 108–114. [[CrossRef](#)] [[PubMed](#)]
11. Edge, R.; Truscott, T.G. Singlet Oxygen and Free Radical Reactions of Retinoids and Carotenoids—A Review. *Antioxidants* **2018**, *7*, 5. [[CrossRef](#)]
12. Rowles, J.L., III; Erdman, J.W., Jr. Carotenoids and their role in cancer prevention. *BBA-Mol. Cell Biol. Lipids* **2020**, *1865*, 158613. [[CrossRef](#)]
13. Park, H.; Hayden, M.M.; Bannerman, S.; Jansen, J.; Crowe-white, K.M. Anti-Apoptotic Effects of Carotenoids in Neurodegeneration. *Molecules* **2020**, *25*, 3453. [[CrossRef](#)] [[PubMed](#)]
14. Alavizadeh, S.H.; Hosseinzadeh, H. Bioactivity assessment and toxicity of crocin: A comprehensive review. *Food Chem. Toxicol.* **2014**, *64*, 65–80. [[CrossRef](#)] [[PubMed](#)]
15. Edge, R.; Mcgarvey, D.J.; Truscott, T.G. The carotenoids as anti-oxidants—A review. *J. Photochem. Photobiol. B Biol.* **1997**, *41*, 189–200. [[CrossRef](#)] [[PubMed](#)]
16. Kuki, M.; Koyama, Y.; Nagae, H. Triplet-Sensitized and Thermal Isomerization of All-Trans, 7-Cis, 13-Cis, and 15-Cis Isomers of beta-Carotene : Configurational Dependence of the Quantum Yield of Isomerization via the T1 State. *J. Phys. Chem.* **1991**, *95*, 7171–7180. [[CrossRef](#)]
17. Rios, A.D.O.; Borsarelli, C.D.; Mercadante, A.Z. Thermal degradation kinetics of bixin in an aqueous model system. *J. Agric. Food Chem.* **2005**, *53*, 2307–2311. [[CrossRef](#)]
18. Hashimoto, H.; Koyama, Y. Time-resolved absorption spectroscopy of the triplet state produced from the all-trans, 7-cis, 9-cis, 13-cis, and 15-cis isomers of β -Carotene. *Chem. Phys. Lett.* **1989**, *162*, 517–522. [[CrossRef](#)]
19. Hashimoto, H.; Koyama, Y. Time-resolved resonance Raman spectroscopy of triplet.beta.-carotene produced from all-trans, 7-cis, 9-cis, 13-cis, and 15-cis isomers and high-pressure liquid chromatography analyses of photoisomerization via the triplet state. *J. Phys. Chem.* **1988**, *92*, 2101–2108. [[CrossRef](#)]
20. Milanowska, J.; Gruszecki, W.I. Heat-induced and light-induced isomerization of the xanthophyll pigment zeaxanthin. *J. Photochem. Photobiol. B Biol.* **2005**, *80*, 178–186. [[CrossRef](#)]
21. Foote, C.S.; Chang, Y.C.; Denny, R.W. Chemistry of singlet oxygen. XI. Cis-trans isomerization of carotenoids by single oxygen and a probable quenching mechanism. *J. Am. Chem. Soc.* **1970**, *92*, 5218–5219. [[CrossRef](#)]
22. Krasnovskii, A.A.; Paramonova, L.I. Interaction of singlet oxygen with carotenoids: Rate constants of physical and chemical quenching. *Biophysics* **1983**, *28*, 769–774.
23. Manitto, P.; Speranza, G.; Monti, D.; Gramatica, P. Singlet oxygen reactions in aqueous solution. Physical and chemical quenching rate constants of crocin and related carotenoids. *Tetrahedron Lett.* **1987**, *28*, 4221–4224. [[CrossRef](#)]
24. Ouchi, A.; Koichi, A.; Iwasaki, Y.; Inakuma, T.; Junji, T.; Nagaoka, S.-I.; Mukai, K. Kinetic Study of the Quenching Reaction of Singlet Oxygen by Carotenoids and Food Extracts in Solution. Development of a Singlet Oxygen Absorption Capacity (SOAC) Assay Method. *J. Agric. Food Chem.* **2010**, *58*, 9967–9978. [[CrossRef](#)] [[PubMed](#)]

25. Speranza, G.; Manitto, P.; Monti, D. Interaction between singlet oxygen and biologically active compounds in aqueous solution III. Physical and chemical $1O_2$ -quenching rate constants of 6,6'-diapocarotenoids. *J. Photochem. Photobiol. B Biol.* **1990**, *8*, 51–61. [[CrossRef](#)]
26. Montenegro, M.A.; Rios, A.D.O.; Mercadante, A.Z.; Nazareno, M.A.; Borsarelli, C.D. Model Studies on the Photosensitized Isomerization of Bixin. *J. Agric. Food Chem.* **2004**, *52*, 367–373. [[CrossRef](#)]
27. Montenegro, M.A.; Nazareno, A.; Durantini, E.N.; Borsarelli, C.D. Singlet Molecular Oxygen Quenching Ability of Carotenoids in a Reverse- micelle Membrane Mimetic System. *Photochem. Photobiol.* **2002**, *75*, 353–361. [[CrossRef](#)]
28. Bors, W.; Michel, C.; Saran, M. Inhibition of the Bleaching of the Carotenoid Crocin a Rapid Test for Quantifying Antioxidant Activity. *Biochim. Biophys. Acta-Lipids Lipid Metab.* **1984**, *796*, 312–319. [[CrossRef](#)]
29. Cerdá-Bernad, D.; Valero-Cases, E.; Pastor, J.; Frutos, M.J. Saffron bioactives crocin, crocetin and safranal: Effect on oxidative stress and mechanisms of action. *Crit. Rev. Food Sci. Nutr.* **2022**, *62*, 3232–3249. [[CrossRef](#)]
30. Hashemzaei, M.; Mamoulakis, C.; Tsarouhas, K.; Georgiadis, G.; Lazopoulos, G.; Tsatsakis, A.; Shojaei, E.; Rezaee, R. Crocin: A Fighter against Inflammation and Pain. *Food Chem. Toxicol.* **2020**, *143*, 111521. [[CrossRef](#)]
31. Naserizadeh, S.K.; Taherifard, M.H.; Shekari, M.; Mesrkanlou, H.A.; Asbaghi, O.; Nazarian, B.; Khosroshahi, M.Z.; Heydarpour, F. The effect of crocin supplementation on lipid concentrations and fasting blood glucose: A systematic review and meta-analysis and meta-regression of randomized controlled trials. *Complement. Ther. Med.* **2020**, *52*, 102500. [[CrossRef](#)]
32. Ali, S.; Davinelli, S.; Mencucci, R.; Fusi, F.; Scuderi, G.; Costagliola, C.; Scapagnini, G. Crosslinked Hyaluronic Acid with Liposomes and Crocin Confers Cytoprotection in an Experimental Model of Dry Eye. *Molecules* **2021**, *26*, 849. [[CrossRef](#)] [[PubMed](#)]
33. Craw, M.; Lambert, C. The characterisation of the triplet state of crocetin, a water soluble carotenoid, by nanosecond laser flash photolyses. *Photochem. Photobiol.* **1983**, *38*, 241–243. [[CrossRef](#)]
34. Chábera, P.; Fuciman, M.; Naqvi, K.R.; Polívka, T. Ultrafast dynamics of hydrophilic carbonyl carotenoids—Relation between structure and excited-state properties in polar solvents. *Chem. Phys.* **2010**, *373*, 56–64. [[CrossRef](#)]
35. Speranza, G.; Dadà, G.; Manitto, P.; Monti, D.; Gramatica, P. 13-cis-crocin: A new crocinoid of saffron. *Gazz. Chim. Ital.* **1984**, *114*, 189–192.
36. Merkel, P.B.; Kearns, D.R. Radiationless Decay of Singlet Molecular Oxygen in Solution. An Experimental and Theoretical Study of Electronic-to-Vibrational Energy Transfer. *J. Am. Chem. Soc.* **1972**, *94*, 7244–7253. [[CrossRef](#)]
37. Manitto, P.; Speranza, G.; Malatesta, V. The quenching of $1O_2$ ($1\Delta_g$) by anthracyclines in aqueous solution. Evidence for a charge-transfer mechanism. *Chem. Phys. Lett.* **1989**, *159*, 310–314.
38. Young, R.H.; Wehrly, K.; Martin, R.L. Solvent effects in dye-sensitized photooxidation reactions. *J. Am. Chem. Soc.* **2002**, *93*, 5774–5779. [[CrossRef](#)]
39. Guo, W.; Tu, C.; Hu, C. Cis—Trans Isomerizations of Carotene and Lycopene: A Theoretical Study. *J. Phys. Chem.* **2008**, *112*, 12158–12167. [[CrossRef](#)]
40. Potashnik, R.; Goldschmidt, C.R.; Ottolenghi, M. Triplet state formation in the quenching of fluorescence by molecular oxygen. *Chem. P* **1971**, *9*, 424–425. [[CrossRef](#)]
41. Zheng, X.; Huang, Q. Assessment of the antioxidant activities of representative optical and geometric isomers of astaxanthin against singlet oxygen in solution by a spectroscopic approach. *Food Chem.* **2022**, *395*, 133584. [[CrossRef](#)]
42. Liu, X.; Osawa, T. Cis astaxanthin and especially 9- cis astaxanthin exhibits a higher antioxidant activity in vitro compared to the all- trans isomer. *Biochem. Biophys. Res. Commun.* **2007**, *357*, 187–193. [[CrossRef](#)] [[PubMed](#)]
43. Saito, I.; Matsuura, T.; Inoue, K. Formation of Superoxide Ion via One-Electron Transfer from Electron Donors to Singlet Oxygen. *J. Am. Chem. Soc.* **1983**, *105*, 3200–3206. [[CrossRef](#)]
44. Pierlot, C.; Hajjam, S.; Barthélémy, C.; Aubry, J.M. Water-soluble naphthalene derivatives as singlet oxygen ($1O_2$, $1\Delta(g)$) carriers for biological media. *J. Photochem. Photobiol. B Biol.* **1996**, *36*, 31–39. [[CrossRef](#)]
45. Ramel, F.; Birtic, S.; Cuiné, S.; Triantaphylidès, C.; Ravanat, J.; Havaux, M. Chemical Quenching of Singlet Oxygen by Carotenoids in plants. *Plant Physiol.* **2012**, *158*, 1267–1278. [[CrossRef](#)]

Disclaimer/Publisher's Note: The statements, opinions and data contained in all publications are solely those of the individual author(s) and contributor(s) and not of MDPI and/or the editor(s). MDPI and/or the editor(s) disclaim responsibility for any injury to people or property resulting from any ideas, methods, instructions or products referred to in the content.